

Ultrashort-Pulse Generation and Ultrafast Phenomena

Sponsors

Joint Services Electronics Program
U.S. Air Force – Office of Scientific Research
U.S. Navy - Office of Naval Research (MFEL)

Project Staff

Andrew Kowalevich, Rohit P. Prasankumar, Dr. Christian Chudoba, Dr. Ingmar Hartl, Dr. Franz X. Kärtner, Dr. Uwe Morgner, Dr. James N. Walpole, Professor Micheal Ruane, Leo J. Misaggia, Paul Mak, Professor Erich P. Ippen, Professor Hermann Haus, and Professor James G. Fujimoto

1. Sources for Ultrashort Pulse Generation

The production of ultrashort laser pulses continues to be a very active field of research. This technology has found applications in the areas of biomedical optics, high speed communications, and the investigation of ultrafast nonlinear processes in semiconductor materials and devices. Generally, these laser sources aim to be cost effective, robust, and technologically simple. Kerr-lens modelocking (KLM), which utilizes the electronic Kerr effect to create an artificial fast saturable absorber, has been the most successful technique for the generation of ultrashort pulses. Working in collaboration with Professors Erich P. Ippen and Hermann A. Haus, we have developed a theoretical model which provides a foundation for understanding and optimizing short-pulse KLM lasers. Our program investigates several areas of ultrafast laser technology, with the objective of developing new technologies that can be applied across a range of laser materials and systems.

Double Chirped Mirror Design

Solid state lasers can have gain over extremely broad bandwidths of several hundred nm, enabling both the generation of few cycle pulse durations or longer pulse durations with broad tunability. Intracavity dispersion is the limiting factor in laser performance for sub-10 fs pulses due to their broad bandwidth. Intracavity prisms have been used for dispersion compensation. However, prisms have parasitic higher order dispersion, which limits pulse duration and also makes laser tuning difficult. Self-phase modulation (SPM) is a temporal nonlinear effect also originating in the Kerr nonlinearity at high intensities that generates new frequencies and spectrally broadens the pulse. When dispersion is carefully compensated, SPM can aid in generation of pulses with spectra that extend beyond the gain bandwidth.

Double chirped mirrors (DCMs) have recently emerged as a powerful technology which permits intracavity dispersion management [1-6] DCMs enable both broadband operation and intracavity dispersion compensation without prisms. Figure 1 shows the differences between standard Bragg mirrors, simple chirped mirrors, and double-chirped mirrors. In a simple chirped mirror the Bragg-wavelength of the grating increases with increasing penetration depth of light into the mirror. Light is reflected at the index discontinuity between the surrounding air and the first layer in the mirror and during chirping of the Bragg-wavelength. These reflections interfere with the strong reflection from the back of the mirror which leads to Gires-Tournois like interferences resulting in strong dispersion oscillations. In a double-chirped mirror we avoid these spurious reflections by a consistent impedance matching from the ambient air all the way to the classical turning point of the wave in the chirped mirror. This is achieved by matching from air to the first low index layer of the actual DCM by a broadband AR-coating. Additional spurious reflections inside the chirped mirror are avoided by slowly switching on the grating, which can be done by increasing the thickness of the high-index layer adiabatically from an almost vanishing value to the corresponding quarter wave thickness. The proper design of DCMs enables the intracavity dispersion to be almost perfectly compensated, removing all higher order dispersion terms over

the laser bandwidth which limit the generation of short pulses. We have recently demonstrated a 5 fs Ti:Al₂O₃ laser where we compensated in average dispersion up to sixth order over one octave of bandwidth [7].

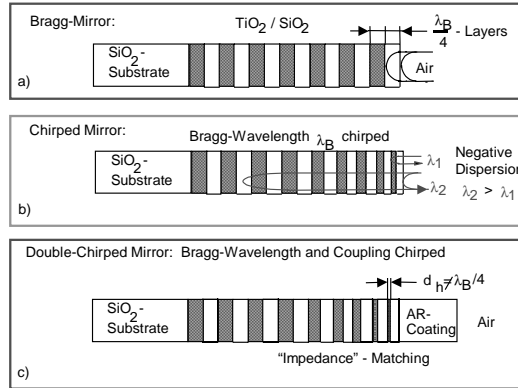


Figure 1: Schematic drawing of layer sequence for various dielectric mirrors: a) standard quarter wave Bragg mirror, b) simple chirped mirror, c) double chirped mirror (DCM).

We have recently developed an analytic theory for the design of dispersion compensating mirrors and mirror pairs [4, 5, 8, 9]. Dispersion compensating mirrors, and especially double-chirped mirrors developed in our group, provide high reflectivity and well controlled dispersion over 400 nm in the case of single mirrors or even over one octave using specially matched mirror pairs. These components are a prerequisite for miniaturized ultrabroadband femtosecond lasers necessary for biomedical optical imaging, ultrafast instrumentation, and other applications.

In our previous work pulses shorter than 5.4 fs at a center wavelength of 800 nm, corresponding to a bandwidth greater than 350 nm, were generated directly by a Kerr-lens mode-locked Ti:sapphire laser at a repetition rate of 90 MHz and an average output power of 200 mW. In this laser, the pulse duration was limited by the bandwidth over which the DCMs can balance the dispersion inside the cavity. The gain bandwidth of Ti:Al₂O₃ extends from 600 nm to almost 1200 nm and would enable the generation of even shorter pulses, in the single-cycle regime. However, increasing the bandwidth of the DCMs results in stronger oscillations of the group delay, which limits the pulse duration. This effect is a consequence of fundamental properties of DCM operation. This problem can be solved by developing complementary sets of mirrors. The phase of the group delay oscillations can be controlled since it depends on the index and layer thickness of the dielectric layers. Two complementary sets of ultra-broadband DCMs can be designed with excess group delay oscillations that are exactly out of phase. Using these two mirror sets, the excess oscillations can be made to cancel. This novel approach enables dispersion compensation over a much greater spectral range than possible using a single mirror set and enables the generation of unprecedented bandwidths and pulse durations. Figure 2 shows the calculated and measured reflectivity and group delay dispersion of the mirror pairs. The mirrors are designed such that the dispersion of all intracavity components is exactly compensated up to sixth-order.

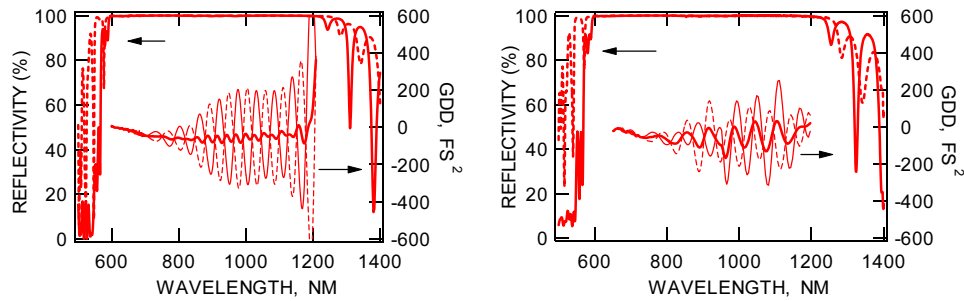


Figure 2: Calculated and measured reflectivity and dispersion of ultrabroad bandwidth DCM pairs specially designed to cancel parasitic dispersion oscillations.

Record Pulse Generation of 5 fs with Octave Bandwidth

Using this novel design, we recently demonstrated the generation of pulses with durations of only 5 fs and spectral bandwidths over one octave directly from a Ti:Al₂O₃ laser [7]. This is the shortest pulse ever generated directly from a laser. Figure 3 shows a schematic of our laser system. This laser has a standard z-cavity design with the addition of a second intracavity fold. A second focus is generated by M4 and M6 in which a 2.4 mm thick plate of BK7 is positioned. This provides enhanced self phase modulation and increases the laser bandwidth.

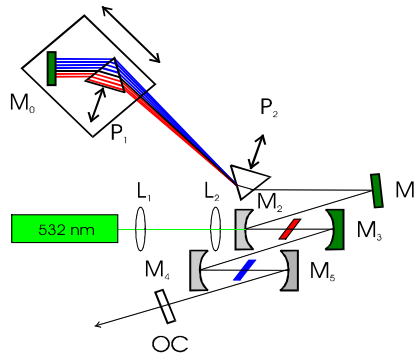


Figure 3: Schematic of Ti:sapphire laser that generates octave bandwidths and 5 fs pulse durations. A second focus was used to increase bandwidth via self phase modulation.

The optical power spectrum at the laser output is displayed in Figure 4(a) on a linear and logarithmic scale. On a log scale the spectrum extends from 600 to 1350 nm above the noise floor. The FWHM of the corresponding pulse assuming a flat phase would be 4.3 fs. The structure in the spectrum is correlated with oscillations in the measured intracavity GDD suggesting that improved DCM design would improve the laser performance. The two peaks at 700 nm and 1050 nm are caused by the increasing output coupling mirror transmission. Despite the large oscillations in the GDD caused by fabrication tolerances, the spectrum is relatively smooth, which can be explained by the enhanced SPM due to the second intracavity focus and the strong KLM action, which continuously cleans up the pulse shape. The interferometric autocorrelation measurement is displayed in Figure 4(b). A phase retrieval algorithm [10] was used to reconstruct the actual pulse shape from the autocorrelation. The intensity envelope of the reconstructed pulse indicates a FWHM of 5 fs. The phase measurement suggests that reductions in duration to 4.5 fs should be possible.

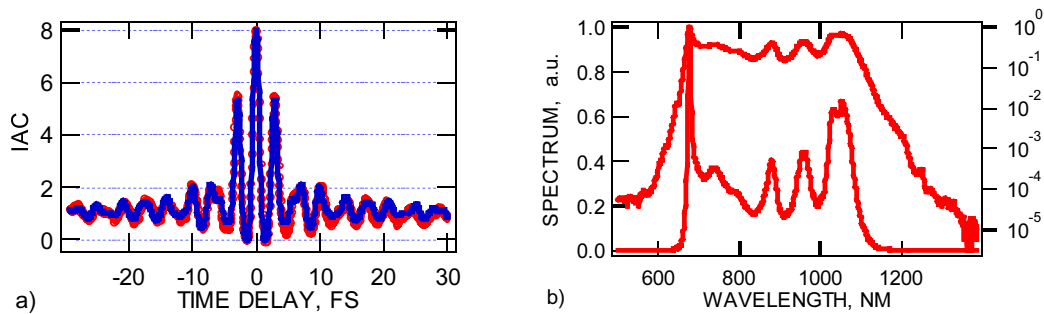


Figure 4: a) Interferometric autocorrelation of the 5 fs pulse b) corresponding spectrum on a linear and logarithmic scale. These are the shortest pulses ever generated directly from a laser.

High performance Cr:Forsterite lasers at 1.3 μm using DCMs

Dispersion management techniques using DCMs can be applied to a wide range of solid state laser materials. The spectral range at 1.3 μm is of particular interest because it falls into the 2nd telecommunication window. Our group recently demonstrated an all-solid-state, Kerr-lens mode-locked Cr:forsterite laser producing 14 fs pulses with 250 nm bandwidth at 1.3 μm using double-chirped mirrors for intracavity dispersion management. An average power of 80 mW at 100 MHz repetition rate was achieved. These pulses are the shortest pulses ever produced by a Cr:forsterite laser [11]. In the 1.3 μm wavelength range, dispersion compensation is particularly challenging because higher order dispersion becomes the dominant factor near the zero dispersion wavelength. Higher order dispersion is hard to compensate over an extended wavelength range even with DCMs. Therefore, it is important to minimize higher order dispersion in the cavity by reducing the crystal length and choosing the optimum prism material. We used PBH71 (SF58) with a zero dispersion wavelength of 2 μm as prism material. This zero dispersion wavelength is much longer than the operating wavelength and results in a favorable ratio of second to third order dispersion in the lasing range and allows broadband DCMs to be fabricated. All mirrors in the cavity are DCMs except for the output-coupling mirror, resulting in 5 bounces on DCMs per round-trip. The DCMs in combination with the PBH71 prisms balance the dispersion in the range from 1.2-1.48 μm . This dispersion compensation results in the broad spectrum with 250 nm bandwidth (FWHM) shown in Figure 5(a) and enables the generation of 14 fs pulses as shown by the interferometric autocorrelation in Figure 5(b).

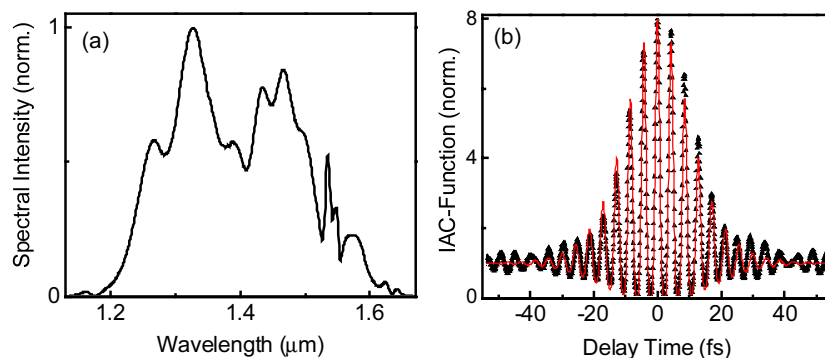


Figure 5: Output spectrum and interferometric autocorrelation of the Cr:forsterite laser showing record 250 nm bandwidth and 14 fs pulse duration.

2. Nonepitaxially Grown Saturable Absorber Materials for Laser Modelocking

Semiconductor saturable absorbers are a widely used technology for generating femtosecond pulses in solid state lasers, providing advantages such as self-starting operation and the potential for compact laser cavities. The most common semiconductor saturable absorber devices are fabricated by molecular beam epitaxy (MBE) and have been used for both saturable absorber modelocking and initiation of Kerr lens modelocking (KLM) in many solid state laser systems [12, 13]. However, MBE has disadvantages including high complexity and cost as well as lattice matching constraints that limit material choice.

Recently we have developed non-epitaxially grown saturable absorber devices and applied them to self-starting KLM in a Ti:Al₂O₃ laser [14]. The devices consist of InAs nanocrystallites doped into SiO₂ films in a 10%InAs/90%SiO₂ ratio and deposited on sapphire substrates using a non-magnetron radio frequency (RF) sputtering system. Advantages of this method include low cost and flexibility in choice of the semiconductor dopant and substrate materials. Rapid thermal annealing (RTA) from 500-750 °C was used to control the absorption saturation dynamics. The structural and optical properties of the devices were comprehensively characterized [15] and the devices were used to initiate KLM in a Ti:Al₂O₃ laser. Self-starting 25 fs pulses were obtained with a bandwidth of 53 nm and tuning range of 80 nm. The saturation fluence of these devices was measured to be 25 mJ/cm², which is too high to enable saturable absorber modelocking without KLM and also limits the minimum achievable pulsewidth.

Recently, we have investigated different approaches to reducing the saturation fluence of our non-epitaxially grown saturable absorbers. We have developed a novel pump-probe system using a broadband 5.5 fs Ti:Al₂O₃ laser [6] to obtain 17 fs time resolution and independent pump and probe wavelength tunability over a range of 700 to 1000 nm. Using this system, we have characterized the nonlinear optical properties of our non-epitaxially grown semiconductor-doped silica film saturable absorbers and discovered trends that aid in device optimization. The devices used in this study were fabricated with a magnetron RF sputtering system, while varying growth parameters such as InAs/SiO₂ ratio and substrate temperature. Degenerate pump-probe experiments on 10%InAs/90%SiO₂ films at wavelengths between 750 and 925 nm (Figure 6) indicate that operation closer to the absorption edge results in lower saturation fluences.

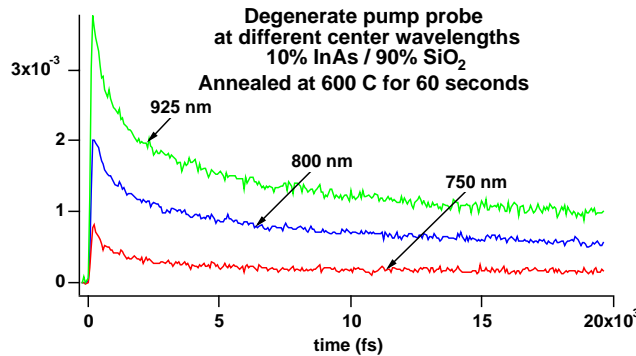


Figure 6: Tunable pump probe measurements between 750 and 900 nm revealing a decrease in saturation fluence with wavelength.

Using this guideline, InAs-doped silica film saturable absorbers with an InAs/SiO₂ ratio of 40%/60% were fabricated. Linear transmission measurements reveal the absorption edge to be redshifted, implying larger quantum dot size in the films. These devices were then characterized in the 1.43-1.54 μm wavelength range using an optical parametric oscillator based pump-probe system (Figure 7). It is clear from these measurements that the saturation fluence of these devices decreases with operation closer to the bandedge, as expected from the earlier

measurements. The lowest saturation fluence of 2 mJ/cm^2 was obtained at $1.5 \mu\text{m}$, where the lasing wavelength is closest to the absorption edge. This is significantly lower than the saturation fluence at 800 nm for $10\% \text{InAs}/90\% \text{SiO}_2$ films and could enable saturable absorber modelocking without KLM in Cr:forsterite or Cr:YAG lasers while also self-starting KLM.

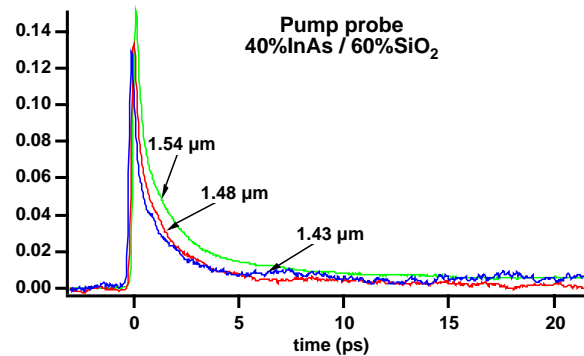


Figure 7: Pump-probe measurements between $1.43 \mu\text{m}$ and $1.54 \mu\text{m}$ on annealed $40\% \text{InAs} / 60\% \text{SiO}_2$ films.

We investigated the application of these devices to self-starting modelocking in a Cr:forsterite laser operating at $1.25 \mu\text{m}$. This laser, as described above, produces 14 fs pulses in a standard 4 mirror configuration. The cavity was modified (Figure 8) to include an additional fold for focusing onto the saturable absorber in a transmissive geometry. Using films with a $40\%/60\%$ InAs/SiO₂ ratio that were designed to have 1% absorption at $1.25 \mu\text{m}$, self-starting KLM was obtained, with a bandwidth of 91 nm and a pulsewidth of 30 fs measured by interferometric autocorrelation. We are currently optimizing the system for minimum pulsewidth and best self-starting performance.

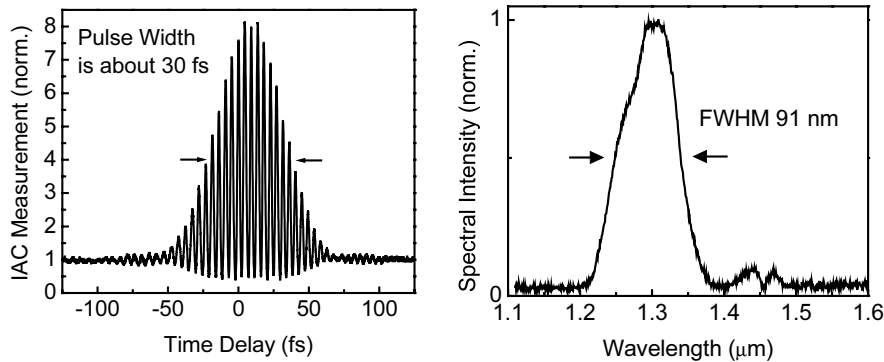


Figure 8: Self-starting KLM in Cr:forsterite using $40\% \text{InAs}/60\% \text{SiO}_2$ semiconductor-doped silica films.

3. Micromachined Photonic Devices using Nonlinear Materials Processing

Photonic device fabrication using nonlinear material processing with near-IR femtosecond pulses has several advantages. Localized, clean, three-dimensional structures can be created in many materials such as bulk glasses [16-18]. Although the mechanism of the nonlinear processing in glass is still under investigation, a variety of devices have been successfully demonstrated and this technique has become an active area of research [19-24]. Laser amplifier systems had been required to reach the high intensities necessary for the nonlinear interaction. Very recently, the processing of glass waveguides using pulses directly from femtosecond lasers oscillators, without the need for amplification, has been reported [25, 26]. Oscillators are more convenient and more cost effective than amplifier systems, and moreover, their higher repetition rate enable faster and

more efficient fabrication. Because oscillators have MHz repetition rates, multiple pulses interact with the same sample volume, and the mechanism for materials processing can differ from amplified pulses at kHz rates. In addition to superposing the effects of each pulse, investigators have reported that cumulative heating occurs when successive pulses interact within a microsecond time scale. Device properties strongly depend on the exposure parameters. The optical properties and dimensions of structures can be controlled by varying the laser pulse duration, focal spot size, scan speed, i.e., number of pulses, and incident power. However, careful investigation and characterization of the effects of exposure parameters on the fabrication are required. In our previous study, a high-power femtosecond Ti:Al₂O₃ laser oscillator using a novel long cavity design was developed which can generate pulse energies far above the threshold for nonlinear processing in glass [27, 28]. This enables greater flexibility in incident power, focus, and processing speed, which is important for fabricating complex devices as well as for device characterization because precise manipulation of structures and optical properties is required. It also enables the fabrication of a wider variety of materials. In this year's report, we demonstrate fabrication and characterization of photonic devices in glass using unamplified pulses from a femtosecond oscillator. Optical coherence tomography is used to measure waveguide structure and refractive index changes. Variable coupling ratio X couplers are demonstrated.

The laser source used for these studies is a long cavity Kerr lens mode locked Ti:Al₂O₃ laser pumped by an Ar⁺ laser. The laser uses a multiple pass cavity formed by a Herriott type cell to extend the cavity length, reducing the repetition rate and increasing the output pulse energy. The laser generates pulses of 80 fs width and 4 MHz repetition rate with a maximum energy of 100 nJ at 800 nm, operating in the standard negative dispersion regime using a saturable Bragg reflector (SBR) for stabilizing the modelocking. The femtosecond pulses from the oscillator were tightly focused inside a 1 mm glass plate (Corning 0215 glass) using a microscope objective. The absorption edge of the glass was approximately 300 nm. Waveguides were fabricated by translating the sample.

We fabricated waveguides and characterized the waveguide size and mode structure as a function of the incident pulse energy and scan speed. In order to investigate the guided mode properties, we cut and polished both ends of the waveguides, coupled a single mode He-Ne laser beam at 633 nm wavelength, and monitored the near field and far field output patterns with a CCD camera. Single mode waveguides of 4.6 μm width could be fabricated by exposure to pulse energies of typically 20 nJ with 80 fs pulse duration and 4 MHz repetition rate, scanning at a speed of 10 mm/s. In contrast, when the exposure power was very high or scanning speed was slow, void-like structures were observed. By using a combination of different laser exposures, it should be possible to fabricate integrated systems with different structures.

The change in refractive index which can be achieved using a given laser exposure is an important parameter for device design. We measured the refractive index differentials using optical coherence tomography (OCT) [29]. A schematic of the measurement is shown in Figure 9. Because of the small dimensions of the waveguides, ultrahigh resolution OCT measurements were required to resolve the waveguide structure [30]. Broadband, low coherence light from a Ti:Al₂O₃ laser with 250 nm bandwidth at 800 nm was focused on the top and bottom interfaces of the waveguide and the back reflected light was interfered with light traversing a reference path. A cross sectional OCT image was constructed by scanning of the reference delay and the sample position.

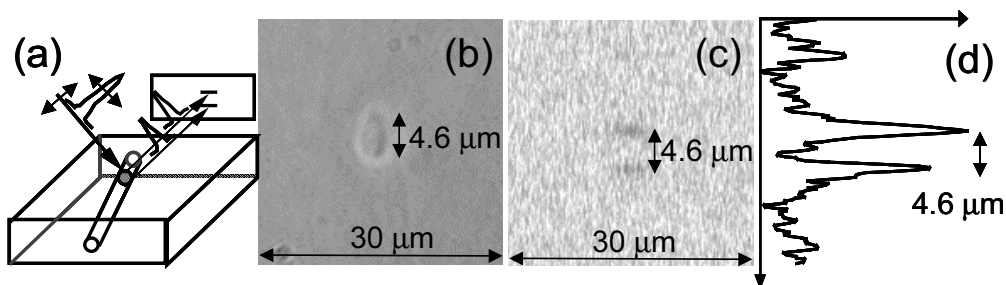


Figure 9: a) Schematic of OCT measurement. Images b) and c) show a side view of the single mode waveguide and the corresponding OCT image. The reflections from the top and bottom boundaries of the waveguide are clearly resolved in the OCT image d).

The refractive index change can be obtained by measuring the magnitude of the reflected signal from the top and bottom interfaces of the waveguide. The refractive index change inside the waveguide was estimated as $\Delta n \sim 0.7 \times 10^{-3}$. When the fabrication parameters were changed, increasing exposure, the maximum index change observed increased to $\Delta n \sim 9 \times 10^{-3}$. As a consistency check, the refractive index inside the waveguide was also estimated using guided mode analysis. By changing fabrication parameters, such as exposure power and scanning speed, a range of waveguide sizes could be fabricated. We estimated the single mode cut-off radius to be in the range of 2 to 4 μm , and calculated the range of the refractive index differential to be $\Delta n \sim 1 \times 10^{-3}$ to 5×10^{-3} . Further investigation of the effects of exposure parameters is required, however, it is important to note that OCT and guided mode analysis gave consistent results.

With the development of single mode waveguides, it is possible to fabricate a wide range of devices. As a starting point, we demonstrated the fabrication of an X coupler. The X coupler was fabricated by writing two identical waveguides with a 1-degree crossing angle. Figure 10(a) shows a top view of the X coupler using a phase contrast microscope with a 10x objective. The total lengths of the waveguides are 7 mm, and the separations of the two waveguide branches at the ends are 90 μm . When a cw Ti:Al₂O₃ laser beam at 800 nm was coupled into one of the input ports, two output spots were observed. The far field pattern of the output beam from one of the output ports is shown in Fig. 10(b). Cross sectional profiles of the near field modes at two output ports (open circles) are shown in Fig. 10(c), together with their best-fit Gaussian (lines). The figure demonstrates single mode coupling between the two waveguides. The splitting ratio of the X coupler is approximately 1:1. The coupling ratio can be adjusted by varying the crossing angle of the guides and other waveguide fabrication parameters. An X coupler with a 4-degree waveguide crossing angle had a coupling ratio of 16:1 (with most of the power not transferred to the crossed guide).

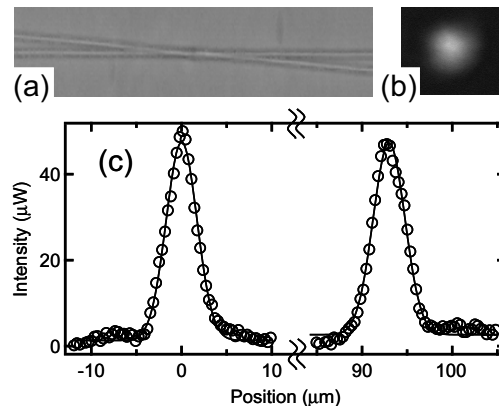


Figure 10: a) Top view of X coupler b) far-field pattern from one of the output ports, c) cross sectional profiles of near field modes at two output ports.

In order to investigate the device properties in detail, we measured the structure of an X coupler using OCT as shown in Figure 11. The OCT images clearly show the internal structure of the device. At the intersection where the two waveguides cross, the reflected signal becomes stronger than from other parts of the waveguide. This shows that the refractive index difference at the waveguide intersection is higher because this portion of the waveguide has been exposed to the laser beam twice. These studies show that OCT can be used to characterize the structure and refractive index differentials of waveguides.

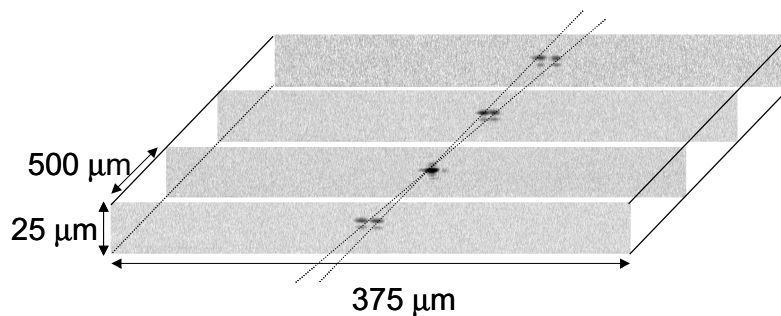


Figure 11: Cross sectional view of X coupler measured using OCT.

One important advantage of device fabrication using femtosecond nonlinear materials processing is that three-dimensional structures can be fabricated. Multiple layers of waveguides can be fabricated to achieve high densities that would not be possible in planer fabrication. In addition, more complex devices which use mode coupling in multiple dimensions can be fabricated. The ability to fabricate in three dimensions should greatly enhance the range of devices which can be developed. We demonstrated the fabrication of a three dimensional device, where waveguides are stacked in multiple layers separated by $\sim 10 \mu\text{m}$, as shown in Figure 12. Using the same focal parameters, waveguides could be fabricated at depths up to $300 \mu\text{m}$ below the surface of the glass.

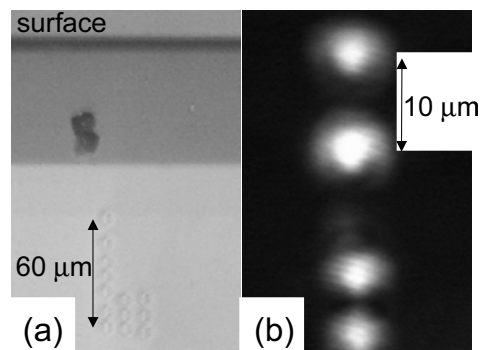


Figure 12: a) Three dimensional device showing waveguides stacked in multiple layers separated by $\sim 10 \mu\text{m}$, b) nearfield pattern of the waveguides with a He-Ne laser coupled into one of the guides, suggesting mode coupling between the 3 dimensional waveguide structures.

This technology is promising for the rapid prototyping and development of new 3D photonic devices and should achieve significantly higher density compared to planer device fabrication.

References

1. Szipöcs, K. Ferencz, C. Spielmann and F. Krausz, "Chirped multilayer coatings for broadband dispersion control in femtosecond lasers," *Optics Letters* 19:(3)p.201-3, 1994.
2. Szipöcs, R., A. Stingl, C. Spielmann and F. Krausz. "Chirped dielectric mirrors for dispersion control in femtosecond laser systems," presented at the in Generation, Amplification, and Measurement of Ultrashort Laser Pulses II, Proc. SPIE, 1995. 6-7 Feb. 1995, San Jose, California.

3. Szipöcs, R. and A. Kohazi-Kis, "Theory and design of chirped dielectric laser mirrors," *Appl. Physics B* 65: p. 115-136, 1997.
4. Kärtner, F. X., N. Matuschek, T. Schibli, U. Keller, H.A. Haus, C. Heine, R. Morf, V. Scheuer, M. Tilsch and T. Tschudi, "Design and fabrication of double-chirped mirrors," *Optics Letters* 22(11): p. 831-33, 1997.
5. Matuschek, N., F.X. Kärtner and U. Keller, "Theory of Double-Chirped Mirrors," *IEEE J. of Sel. Topics in Quantum Electronics* 4(2): p. 197, 1998.
6. Morgner, U., F.X. Kaertner, S.H. Cho, Y. Chen, H.A. Haus, J.G. Fujimoto, E.P. Ippen, V. Scheuer, G. Angelow and T. Tschudi, "Sub-two-cycle pulses from a Kerr-lens mode-locked Ti:sapphire laser," *Optics Letters* 24(6): p. 411-13, 1999.
7. Ell, R., U. Morgner, F.X. Kärtner, J.G. Fujimoto, E.P. Ippen, V. Scheuer, G. Angelow and T. Tschudi, "Generation of 5 fs pulses and octave-spanning spectra directly from a Ti:sapphire laser," *Optics Letters* 26(6): p. 373-5, 2001.
8. Matuschek, N., F.X. Kärtner and U. Keller, "Analytic design of double-chirped mirrors with custom tailored dispersion characteristics," *IEEE J. of Quantum Electronics* 5: p. 129 -- 137, 1999.
9. Kärtner, F.X., U. Morgner, T.R. Schibli, E.P. Ippen, J.G. Fujimoto, V. Scheuer, G. Angelow and T. Tschudi, "Ultrabroadband double-chirped mirror pairs covering for single cycle pulses," *submitted to J. of the Optical Soc. of America B* 2001.
10. Baltuska, A., M. Pugzlys, M. Pshenichnikov, D. Wiersma, B. Hoenders and H. Ferwerda. "How to retrieve amplitude and phase from autocorrelation and spectrum," presented at the Ultrafast Optics, 1999. Ascona, Switzerland.
11. Chudoba, C., J.G. Fujimoto, E.P. Ippen, H.A. Haus, U. Morgner, F.X. Kärtner, V. Scheuer, G. Angelow and T. Tschudi, "All-solid-state Cr:forsterite laser generating 14 fs pulses at 1.3 μm ," *Optics Letters* 26: p. 292 - 294, 2001.
12. Keller, U., K.J. Weingarten, F.X. Kaertner, D. Kopf, B. Braun, I.D. Jung, R. Fluck, C. Honninger, N. Matuschek and J.A.D. Au, "Semiconductor saturable absorber mirrors (SESAM's) for femtosecond to nanosecond pulse generation in solid-state lasers," *IEEE Journal of Selected Topics in Quantum Electronics* 2: p. 435-453, 1996.
13. Tsuda, S., W.H. Knox, S.T. Cundiff, W.Y. Jan and J.E. Cuningham, "Mode-locked ultrafast solid-state lasers with saturable Bragg reflectors," *IEEE Journal of Selected Topics in Quantum Electronics* 2: p. 454-464, 1996.
14. Bilinsky, I.P., J.G. Fujimoto, J.N. Walpole and L.J. Misaggia, "Semiconductor-doped silica saturable absorber films for solid state laser mode locking," *Optics Letters* 23: p. 1766-1768, 1998.
15. Bilinsky, I.P., R.P. Prasankumar and J.G. Fujimoto, "Self-starting mode locking and Kerr-lens mode locking of a Ti:al₂O₃ laser by use of semiconductor-doped glass structures," *Journal of the Optical Society of America B* 16: p. 546-549, 1999.
16. Davis, K.M., K. Miura, N. Sugimoto and K. Hirao, "Writing waveguides in glass with a femtosecond laser," *Optics Letters* 21: p. 1729-1731, 1996.
17. Miura, K., J. Qiu, H. Inouye, T. Mitsuyu and K. Hirao, *Applied Physics Letters* 71: p. 3329, 1997.
18. Varel, H., D. Ashkenasi, A. Rosenfeld, M. Waehmer and E.E.B. Campbell, *Applied Physics A* 65: p. 367, 1997.
19. Kondo, Y., K. Nouchi, T. Mitsuyu, M. Watanabe, P.G. Kazansky and K. Hirao, *Optics Letters* 24: p. 646, 1999.
20. Glezer, E.N., M. Milosavljevic, L. Huang, R.J. Finlay, T.H. Her, J.P. Callan and E. Mazur, *Optics Letters* 21: p. 2023, 1996.
21. Glezer, E.N. and E. Mazur, *Applied Physics Letters* 71: p. 882, 1997.
22. Homoelle, D., S. Wielandy, A.L. Gaeta, N.F. Borrelli and C. Smith, "Infrared photosensitivity in silica glasses exposed to femtosecond laser pulses," *Optics Letters* 24: p. 1311-1313, 1999.
23. Cho, S.H., H. Kumagai, K. Midorikawa and M. Obara, *Optics Communications* 168: p. 287, 1999.

24. Sikorski, Y., A.A. Said, P. Bado, R. Maynard, C. Florea and K.A. Winick, "Optical waveguide amplifier in Nd=doped glass written with near-IR femtosecond laser pulses," *Electronic Letters* 36(226)2000.
25. Schaffer, C.B., A. Brodeur, J.F. Garcia and E. Mazur, *Optics Letters* 26: p. 93, 2001.
26. Streltsov, A.M. and N.F. Borrelli, *Optics Letters* 26: p. 42, 2001.
27. Cho, S.H., B.E. Bouma, E.P. Ippen and J.G. Fujimoto, "Low-repetition-rate high-peak power Kerr-lens mode-locked Ti:Al₂O₃ laser with a multiple-pass cavity," *Optics Letters* 24: p. 417-419, 1999.
28. Cho, S.H., F.X. Kaertner, U. Morgner, E.P. Ippen and J.G. Fujimoto, *Optics Letters* .
29. Huang, D., E.A. Swanson, C.P. Lin, J.S. Schuman, W.G. Stinson, W. Chang, M.R. Hee, T. Flotte, K. Gregory, C.A. Puliafito and F. J.G., "Optical Coherence Tomography," *Science* 254: p. 1178, 1991.
30. Drexler, W., U. Morgner, R.K. Ghanta, F.X. Kärtner, J.S. Schuman and J.G. Fujimoto, "Ultrahigh resolution ophthalmic optical coherence tomography," *Nature for Medicine* 7(4): p. 502-7, 2001.

Publications

1. C. Chudoba, J. G. Fujimoto, E. P. Ippen, H. A. Haus, U. Morgner, F. X. Kärtner, V. Scheuer, G. Angelow, and T. Tschudi, "All solid-state Cr:forsterite laser generating 14 fs pulses at 1.3 μm ," *Optics Letters* 26:292-294, March 2001.
2. S. H. Cho, F. X. Kärtner, U. Morgner, E. P. Ippen, J. G. Fujimoto, J. E. Cunningham, W. H. Knox, "90 nJ pulse generation using a 4 MHz repetition rate KLM Ti:Al₂O₃ laser operating with net positive and negative intracavity dispersion," *Optics Letters* 26:560-562, April 2001.
3. R. Ell, U. Morgner, F. X. Kärtner, J. G. Fujimoto, E. P. Ippen, V. Scheuer, G. Angelow, T. Tschudi, M. J. Lederer, A. Boiko, and B. Luther-Davies, "Generation of octave filling spectra, 5-fs-pulses directly from a Ti:Sapphire oscillator with enhanced dispersion-managed-soliton formation," *Optics Letters* 26:373-375, March 2001.